Optimal Energy Requesting Strategy for RF-based Energy Harvesting Wireless Communications

Yu Luo*, Lina Pu*, Yanxiao Zhao*, Guodong Wang* and Min Song†
*Electrical & Computer Engineering, South Dakota School of Mines and Technology, SD, USA 57701
†Computer Science, Michigan Technological University, MI, USA 49931
Email: {yu.luo, lina.pu, yanxiao.zhao, guodong.wang}@sdsmt.edu, mins@mtu.edu

***Abstract*— Energy harvesting is emerging as a promising alternative source to power the next generation of wireless networks. This paper introduces a new energy harvesting strategy that uses a dedicated energy source to optimally replenish energy for radio frequency (RF) based wireless communication systems. Specifically, we develop a two-step dual tunnel energy requesting (DTER) strategy that allows an energy harvesting device to effectively obtain energy from a dedicated energy source. While minimizing the system energy consumption, DTER takes into account the practical constraints on both the energy source and the energy harvesting device. Additionally, the overhead issue and the charge characteristics of an energy storage component are examined to make the proposed strategy practical. To solve the nonlinear optimization problem in DTER, we convert the design of optimal energy requesting problem into a classic shortest path problem and thus enable us to find a global optimal solution through dynamic programming algorithms. Theoretical analysis and simulation study verify that DTER outperforms two other schemes in the literature.**

I. Introduction

Energy harvesting (EH) is considered as a favorable alternative to supply power for the future wireless networks due to several key advantages (i.e., energy self-sustainability, long life time, and pollution free). With the EH technique, an energy harvesting device (EHD) is capable of receiving energy from nature or man-made sources, such as solar, wind or even ambient RF signals, for communications [1]. Along with the remarkable progress on ultra-low power semiconductors, RF-based EH communications have drawn considerable attention in recent years [2]–[4].

The existing RF-based EH systems can be classified into two categories: *without a dedicated energy source* (ES) and *with dedicated ESs*. In the first category, EHDs harvest energy passively from ambient noises of radio frequency (RF), which are radiated from TV towers, access points (APs), or base stations [5], [6]. The performance of a system in this category can be improved by optimizing the data rate and transmission power of EHDs. The activities of ESs, however, are uncontrollable due to a lack of interaction between EHDs and ESs. In the second category, a dedicated ES is installed to power the entire EH network [7]–[9]. In this category, EHDs are allowed to request energy from the associated ES on demand. The replenishment of energy storage components, which is also referred to as battery charging, thus can be scheduled by the ES based on the energy consumption of each EHD.

Current research on RF-based EH communications mainly focuses on improving the utilization of the harvested energy from RF ambient noise. Several policies for power management have been proposed to maximize the energy utilization on EHDs for a perpetual and uninterrupted operation [10]–[13]. The investigation on EH communications with a dedicated ES, by contrast, is still in its initial stage. Actually, the EH systems with a dedicated ES like passive RF identification (RFID) have already been penetrating our daily lives [14], [15]. A number of advanced power supply methods, such as multi-hop energy packet transmission and sharp beamforming energy transfer, are also investigated or tested through theoretical analysis and experiments [7], [8], [16], [17]. How to manage the power at EHDs and schedule the energy transfer at ESs to minimize the overall energy consumption, however, is currently missing and is the focus of this paper.

Intuitively, an RF-based EH system could achieve a satisfactory performance in terms of transmission rate, packet loss and reliability by allowing an EHD to request the energy freely from a dedicated ES. The energy efficiency with such a greedy strategy, however, will be reduced considerably. Specifically, due to the overhead on requesting energy and the nonlinear charging feature of batteries, the energy consumption of an ES system varies dramatically when different energy harvesting strategies are applied. As will be revealed in this paper, if an inappropriate strategy is employed, a large amount of energy is wasted either on sending superfluous request messages or on an inefficient charging process. How to minimize the overall energy consumption while guaranteeing successful data transmission for wireless communications remains a challenge.

In this paper, we propose a two-step dual tunnel energy requesting (DTER) strategy. The objective is to minimize the energy consumption at both the EHD and the ES on transmitting the arrived data timely. DTER is an offline strategy, which means that the EHD is assumed to know exactly the arriving time and the size of future data. The proposed strategy is operated in two steps. The first step derives the profile of optimal transmission rate in a feasible *data tunnel* at an EHD under a data storage constraint. The second step designs a global optimal strategy for energy harvesting in a feasible *energy tunnel* based on the first step subject to the constraint of limited battery capacity. We provide in-depth theoretical analysis, which verifies that the EHD consumes the minimum energy to send all arrived data with the transmission rate obtained from the first step of DTER, as well as the ES charges the EHD most efficiently when applying the energy requesting strategy designed from the second step of DTER.

To summarize, by using DTER, an EHD is able to harvest energy from a dedicated ES timely and efficiently with the minimum energy consumption for both the EHD and the ES.

The contributions of our work is threefold. First, we design an optimal energy requesting strategy under the constraints of data and energy storage capacities to minimize the energy consumption while carefully considering the charging feature of real batteries and the overhead issue in a practical EH system. Second, our offline solution provides a lower bound of the energy consumption at both the EHD and the ES for the EH system with a dedicated ES. Last, our study on the energy requesting problem fills the gap between the dedicated ES based EH communications and the efficient power management.

The remainder of the paper is organized as follows. We introduce the related work in Section II and the system model in Section III. Section IV discusses the first step of DTER to obtain the optimal transmission rate of an EHD. Two important concepts used in the second step of DTER are described in Section V. We study how to design an optimal energy requesting strategy to minimize the overall energy consumption in Section VI. Section VII presents simulation results. Conclusions are drawn in Section VIII.

II. Related Work

As a promising technique to build the next generation of green and self-sufficient wireless networks, the EH system without a dedicated ES has been extensively investigated. Many policies are proposed at the EHD side to manage the harvested energy efficiently after considering the intermittency and the randomness of energy arrivals [10]–[13]. Reference [10] introduces an optimal power control policy that minimizes the completion time of transmitting a certain amount of data under an energy storage constraint. The results demonstrate that it is optimal when the transmission power is constant between the arrivals of energy packets. In [11], both the constraints of energy and data storage capacities are taken into account to maximize the short-term throughput of an EHD. The optimal transmission power is shown to be the tightest string that lies in a feasible energy tunnel. The authors in [12] considers the processing costs and energy causality in EH systems, and designs a directional glue pouring algorithm to obtain the optimal transmission policy. In [13], an optimal operation strategy that provides service differentiation among different traffic patterns is proposed, subject to the constraints of data storage capacity and packet loss ratio. To maximize the weighted throughput in the long term, the activity of an EH node is modeled as a constrained Markov decision process and the optimal decision on whether to harvest energy or to send data is figured out.

Although harvesting ambient RF energy solely from surrounding environments to power EHDs is attractive, recent research studies have demonstrated that the transmission rate, reliability, transmission range, and deployment of such devices are extremely limited by the thin energy in the atmosphere [5], [6], [18]. To meet communication requirements (e.g., reliability, delay, and throughput), powering EHDs with a dedicated ES is promoted as an alternative.

References [7] and [8] conduct several experiments studying the RF energy transfer from a dedicated ES to an EHD through multiple hops. The results show that with an optimal placement of relay nodes, a multi-hop scheme could save energy on ES and reduce the time consumption on energy harvests as well. Reference [16] proposes a system for power transfer on an autonomous radio frequency. It is capable of rotating the base of ES to track the position of EHDs and transferring power to a particular device. In [17], the authors advocate the use of massive multiple-input and multiple-output (MIMO) for efficient wireless energy transfer. More specifically, a large-scale antenna array with millimeter-wave (mmWave) enables a sharp beamforming to suppress the propagation loss of energy packets. The authors in [19] propose a CSMA/CA based medium access control protocol for re-chargeable sensor network to schedule both the energy transmission and data communication in a shared medium; the problem of ES deployment is also explored in this work through experimental study.

From the above introduction we realize that the feasibility, hardware design and applications of an EH system with a dedicated ES have been comprehensively studied in the literature; how to efficiently manage the power at both the ES and the EHD, however, is still an open issue. As will be shown in the paper, inappropriate energy requests at the EHD may significantly increase the energy consumption at the ES. Therefore, the objective of this paper is to design an optimal energy requesting strategy that the EHD could harvest energy from the ES with the minimum energy consumption.

III. System Model

We consider an RF-based EH system with a dedicated ES, from which an EHD requests and harvests energy through RF energy packets. The harvested energy is stored in a battery at the EHD and then utilized for its data transmissions. Assume the energy harvesting and data transmissions use separate antennas and frequency bands, i.e., an EHD could request energy and transmit data simultaneously.

Fig. 1 illustrates the energy request problem. Three curves, labeled by L1, L2, and L3, represent the cumulative transmitted energy by the ES, the accumulation of harvested energy and energy consumption at the EHD, respectively. The harvested energy is considered as discrete energy packets with different sizes [10]–[13]. Therefore the profile of harvested energy at the EHD (i.e., L2) is modeled as a staircase curve. As shown in Fig. 1, the EHD initiates the i^{th} energy request at instance t_{r_i} and harvests E_i^r energy in the next T_i^{es} seconds. Here, T_i^{es} is the duration of the energy packet, which is also the charge time for the i^{th} energy request. Assume the ES consumes E_i^{es} energy on transmitting the i^{th} energy packet. Due to the energy loss on propagation and charging, the harvested energy E_i^r is always smaller than the transmitted energy E_i^{es}.

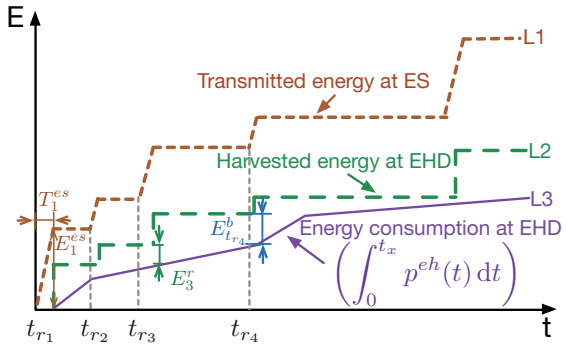

Fig. 1. System model of energy request.

As for data transmissions, an offline scenario is assumed, which means that the EHD knows exactly the arriving time and the size of the n^{th} data packet, denoted by t_{d_n} and D_n, respectively. Let D_m^{eh} be the maximum capacity of data storage and D_t^b be the residual data of the EHD at instance t. The transmission rate of the EHD at time t is represented by $r^{eh}(t)$, which is related to the transmission power, $p^{eh}(t)$, through a power-rate function $r^{eh}(t) = g(p^{eh}(t))$. In general, $g(\cdot)$ is non-negative, increasing, and strictly concave[1]. An illustration of the cumulative energy consumption on data transmission at an EHD, $\int_0^{t_x} p^{eh}(t)\,\mathrm{d}t$, labeled by L3, is shown in Fig. 1.

Let T be the deadline that the EHD sends out all data. Denote the residual energy of the EHD at time $t_x \in [0, T]$ by $E_{t_x}^b$, where

$$E_{t_x}^b = \sum_{k=1}^{t_{r_k}<t_x} E_k^r - \int_0^{t_x} p^{eh}(t)\,\mathrm{d}t. \tag{1}$$

According to the charging characteristic of batteries, the amount of energy to be transmitted by an ES depends not only on the amount of energy to replenish but also on the residual energy at the EHD. The relation between E_i^{es}, E_i^r and $E_{t_{r_i}}^b$ can be represented by $E_i^{es} = z(E_i^r, E_{t_{r_i}}^b)$, where $z(\cdot)$ is called the charging function and the details will be further elaborated in Section V.

The overall objective of this study is to optimize the energy consumption of the ES under the constraints of data and energy storage capacities at the EHD. This optimization problem, denoted by **P1**, is formulated as follows.

$$\begin{aligned}
&\mathbf{P1}: \quad \arg\min_{t_{r_i}, E_i^r} \sum_{i=1}^{t_{r_i}<T} \left(E_i^{es} + e^r\right), \\
&\textbf{s.t.} \\
&\textit{C1}: \int_0^{t_x} p_o^{eh}(t)\mathrm{d}t \le \sum_{i=1}^{t_{r_i}<t_x} E_i^r, \qquad t_x \in [0, T], \\
&\textit{C2}: \; E_{t_x}^b \le E_m^{eh}, \qquad t_x \in [0, T], \\
&\textit{C3}: \; T_i^{es} \le t_{r_{i+1}} - t_{r_i},
\end{aligned} \tag{2}$$

[1]A typical power-rate function in an additive white Gaussian noise (AWGN) channel is $r^{eh}(t) = \log[1 + h(t)p^{eh}(t)]$, where $h(t)$ is the instantaneous channel response for the link between an EHD and its communicating party.

where $p_o^{eh}(t)$ is the optimal transmission power that allows an EHD to send all data timely and with minimum energy consumption. Correspondingly, the integration of $p_o^{eh}(t)$ represents the least amount of energy required at the EHD; E_m^{eh} represents the battery capacity of an EHD and e^r is a constant overhead at the ES to compensate the EHD for the energy spent on transmitting request messages.

In **P1**, the constraint C1 is that at any time the total energy harvested at the EHD should be no less than the accumulation of the minimum energy it consumed; otherwise the arriving data may overflow the storage. The constraint C2 indicates that the difference between the harvested energy and the expended energy cannot exceed the battery capacity of an EHD, which is referred to as the energy capacity constraint. The constraint C3 is a charging constraint that limits the time interval between two consecutive energy requests. Specifically, as demonstrated in Fig. 1, the i^{th} energy charging takes T_i^{es} seconds, the EHD thus cannot initiate a new energy request until the current battery replenishment ends.

After a further study, we interpret problem **P1** as follows: when and how much energy should an EHD request or harvest from the ES, so that the energy consumption at the source is minimized with the three constraints above? To solve problem **P1**, we propose a two-step energy requesting strategy, DTER, which links the *data transmission* profile at the EHD and the scheduling of *energy transmission* at the ES. Specifically, it is critical to build an analytical relationship between the harvested energy and the energy consumption for data transmissions at the EHD. The latter is determined by the EHD's transmission rate via the power-rate function. Therefore, the first step of DTER is to calculate the optimal transmission rate at the EHD in order to minimize its cumulative energy consumption for data transmission. The profile of optimal transmission rate at the EHD obtained from the first step determines the bounds of an energy tunnel. The second step is to design an optimal energy requesting strategy inside the energy tunnel so that the energy consumption at the ES is minimized as well.

IV. Optimal Transmission Rate

In this section, we present the first step of DTER. The objective is to calculate the profile of the optimal transmission rate at the EHD so that its cumulative energy consumption for data transmission is minimized.

A. Feasible Data Tunnel

Assuming the initial energy at the EHD is infinite, we focus on calculating the optimal transmission rate while considering the data capacity constraint. The energy constraint will be integrated into the second step, as presented in Section VI. We formulate the first step of DTER as an optimization problem, as follows.

$$\textbf{P2:} \quad \arg\min_{r^{eh}(t)} \int_0^T g^{-1}\left(r^{eh}(t)\right)\,\mathrm{d}t,$$

s.t.

$$\textbf{C1:} \quad \int_0^{t_x} r^{eh}(t)\,\mathrm{d}t \le \sum_{n=1}^{t_{d_n}<t_x} D_n, \qquad t_x \in [0,T], \tag{3}$$

$$\textbf{C2:} \quad \int_0^{t_x} r^{eh}(t)\,\mathrm{d}t \ge \sum_{n=1}^{t_{d_n}<t_x} D_n - D_m^{eh}, \quad t_x \in [0,T].$$

Here the problem **P2** is to minimize the energy consumption of the EHD on transmitting all data, subject to two constraints. Constraint C1 reflects the causality of data transmission, i.e., the EHD cannot send data that has not arrived yet. Constraint C2 guarantees that the data arrival does not overflow the data storage. These two constraints construct a feasible data tunnel, as illustrated in Fig. 2. The profile of cumulative data transmitted at the EHD is a continuous line (e.g., curve D1 in Fig. 2) that stays within the feasible data tunnel to satisfy the data causality and storage capacity constrains.

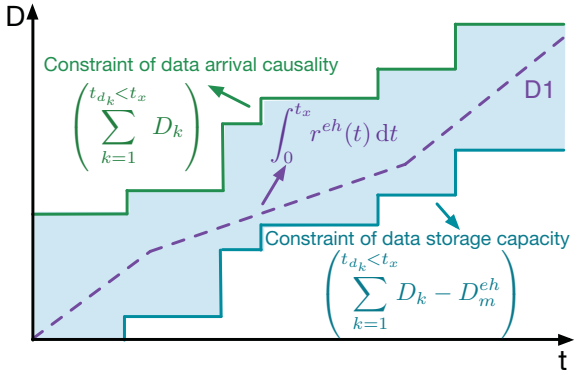

Fig. 2. An example of feasible data tunnel.

B. Lemmas of Optimal Transmission Rate

In this subsection, we present four lemmas to explore the inherent features of the optimal transmission rate, r_o^{th}, in (3).

Lemma 1: *The transmission rate is constant during an interval between the arrivals of two successive data packets.*

Lemma 2: *The transmission rate changes only when the data storage is either full or completely depleted.*

Lemma 3: *The transmission rate decreases monotonically if the data storage is not completely depleted, i.e.,* $\forall\, t_i, t_j \in [0,T], t_i < t_j$: $r_o^{eh}(t_i) \ge r_o^{eh}(t_j)$, *if* $\forall\, t \in [t_i, t_j]$: $D_t^b \ne 0$.

Lemma 4: *The transmission rate increases monotonically if the data storage is not completely filled, i.e.,* $\forall\, t_i, t_j \in [0,T], t_i < t_j$: $r_o^{eh}(t_i) \le r_o^{eh}(t_j)$, *if* $\forall\, t \in [t_i, t_j]$: $D_t^b \ne D_m^{eh}$.

The above lemmas can be proved by the contradiction method. Due to the space limit, the detailed proofs are not provided here. However, similar proofs can be found in [10] and [11].

From Lemma 1 to Lemma 4, the following Corollary is deduced.

Corollary 1: *At instants of data arrival, the transmission rate decreases if the data storage is completely filled or increases if the storage is empty, i.e.,* $\forall\, t \in [0,T]: r_o^{eh}(t^-) > r_o^{eh}(t^+) \Longrightarrow D_t^b = D_m^{eh}$ *and* $r_o^{eh}(t^-) < r_o^{eh}(t^+) \Longrightarrow D_t^b = 0$.

Essentially, the objective of the optimization problem in (3) is to seek the best curve in a feasible data tunnel to minimize a specified cost, which is similar to the optimization problem solved in [11]. Consequently, even though the two optimization problems have entirely different objective functions and constraints, their results are naturally related from the graphical point of view. This can be observed by comparing the above Corollary 1 with Corollary 1 introduced in [11]. To solve **P2**, either the water-filling algorithm presented in [20] or the throughput maximizing method proposed in [11] is a feasible approach. Eventually, it is verified that the profile of the optimal transmission rate, r_o^{eh}, is the tightest and piecewise segments that lie in the feasible data tunnel.

V. Energy Tunnel and Charging Function

Before presenting the second step of DTER, we introduce two concepts first, namely, *feasible energy tunnel* and *charging function*. These two concepts are critical to the design of the second step of DTER (presented in the Section VI) to obtain the optimal strategy for energy harvesting.

A. Feasible Energy Tunnel

The constraints C1 and C2 in problem **P1** define the upper bound and lower bound for the accumulation of harvested energy, respectively. The bounded tunnel is termed the feasible energy tunnel. As illustrated in Fig. 3, the lower bound is the least required power ($\int_0^{t_x} p_o^{eh}(t)$), which can be calculated from the optimal transmission rate (i.e., $r_o^{eh}(t)$) derived from the first step of DTER. The upper bound is obtained by shifting the lower bound up by E_m^{eh}, indicating the battery capacity constraint. As mentioned in Section IV-B, the profile of the optimal transmission rate at the EHD is piecewise linear. Therefore, the feasible energy tunnel is also piecewise linear according to the power-rate function.

The objective in the second step of DTER is to minimize the overall energy consumption of ES, which is achieved by scheduling the stair-stepping profile of harvested energy inside

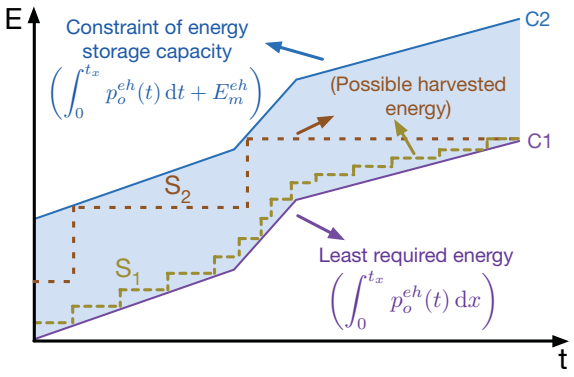

Fig. 3. The feasible energy tunnel.

the feasible energy tunnel, as demonstrated in Fig. 3. Finding the optimal requesting strategy is not trivial. Specifically, the EHD needs to pay a constant cost on each request message transmission, and consequently generates significant energy overhead if it requests too frequently (e.g., curve S1 in Fig. 3). In contrast, requesting a large amount of energy each time will reduce the energy overhead; but the energy cost at the ES increases nonlinearly with the growth of energy to be charged [21] (e.g., curve S2 in Fig. 3). Therefore, neither strategy S_1 nor S_2 is a good option for efficient energy requesting: the former requests energy too frequently, while the latter asks for too much energy in each energy transfer.

B. Charging Function

In RF-based EH systems, an EHD is generally equipped with a super capacitor to store the harvested energy [6], [7], [22]. Therefore, we use the capacitor as an example to provide insight into the charging function, which determines the efficiency of energy replenishment.

To charge an EHD wirelessly, assume the ES transmits energy packets with a constant power, which is represented as p^{es}. Before receiving the i^{th} energy packet at t_{r_i}, denote the voltage and the energy stored in the capacitor of EHD by V_i and $E^b_{t_{r_i}}$, respectively. The transmission time of the energy packet i is T^{es}_i. After the i^{th} energy harvest, the voltage of the capacitor will increase by ΔV_i. According to the definition of the parameters introduced in Section III, we have that

$$\begin{cases} V_i = V_m\left(1-e^{-\frac{t'}{RC}}\right), \\ V_i+\Delta V_i = V_m\left(1-e^{-\frac{t'+T^{es}_i}{RC}}\right), \\ E^b_{t_{r_i}} = \frac{1}{2}CV_i^2, \\ E^b_{t_{r_i}} + E^r_i = \frac{1}{2}C\left(V_i+\Delta V_i\right)^2, \\ E^{es}_i = p^{es}T^{es}_i. \end{cases} \tag{4}$$

In (4), t' is the time consumed on charging the voltage of a capacitor from 0 to V_i with V_m volts of voltage; V_m is the maximum voltage a capacitor could approach, which is determined by the EH circuit and the receiving power of energy packets at an EHD [23], [24]. R and C are the resistance and capacitance of the charging circuit, respectively.

By solving (4), the energy cost on an ES for the i^{th} charging is calculated below:

$$E^{es}_i = p^{es}RC\ln\left\{\frac{\left(2E^{eh}_m\right)^{\frac{1}{2}}-\left(2E^b_{t_{r_i}}\right)^{\frac{1}{2}}}{\left(2E^{eh}_m\right)^{\frac{1}{2}}-\left[2\left(E^b_{t_{r_i}}+E^r_i\right)\right]^{\frac{1}{2}}}\right\}, \tag{5}$$

where $E^{eh}_m = \frac{1}{2}CV^2_m$. The above equation verifies that the energy consumption at ES is not only affected by the amount of energy the EHD claimed, E^r_i, but also by the residual energy in the capacitor, $E^b_{t_{r_i}}$. This phenomenon is also justified in Fig. 4 by the nonlinear charge curve of a real EHD with the capacitor. The data was collected with Powercast P2110 energy harvesting kit [25], where the ES was placed about 1 meter away from the EHD. In the test, the transmission power of the ES was 3 watts; the resistance and the capacity of the capacitor were $4\,\mathrm{k}\Omega$ and $50\,\mathrm{mF}$, respectively. As illustrated in the figure, the variation of capacitor's voltage match the theoretical exponential charge function very well. In addition, it can be observed that if T^{es}_i is fixed, ΔV_i decreases monotonically with the increase of the time, indicating that the efficiency of energy harvest is under the impact of the residual energy in the capacitor.

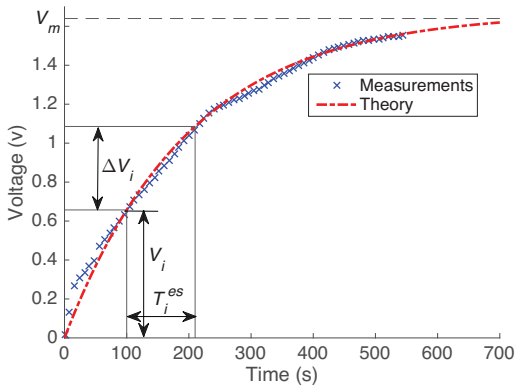

Fig. 4. The charge curve of the capacitor in an EHD, where the theoretical results are calculated through the first equation of (4).

Consequently, it is ready to introduce a useful property of E^{es}_i to support the design of an optimal energy requesting strategy.

Property 1: *E^{es}_i is an increasing function of E^r_i and a strictly convex function of $E^b_{t_{r_i}}$. With regard to E^r_i, the E^{es}_i function is strictly concave if $E^i_r + E^b_{t_{r_i}} \in [0, \frac{1}{4}E^{eh}_m)$, and strictly convex if $E^r_i + E^b_{t_{r_i}} \in [\frac{1}{4}E^{eh}_m, E^{eh}_m]$.*

The verification of Property 1 is straightforward. We can prove it by inspecting the first order and the second order partial derivatives of E^{es}_i in (5) with respect to E^r_i and $E^b_{t_{r_i}}$.

Property 1 and (5) indicate that with a fixed charging time, i.e., the length of energy packets, the energy harvested by an EHD does not decrease monotonically with the increase of $E^b_{t_{r_i}}$. In other words, to improve the efficiency of energy harvest, the EHD needs to keep a certain amount of energy in its capacitor.

VI. Energy Requesting Strategy

The second step of DTER focuses on how to design the optimal strategy for energy requesting. For that, we first investigate the piecewise optimal strategies without the overhead energy, which provides an upper bound of the data transmission rate that a capacitor-based EHD can achieve. Then propose a heuristic approach that converts the scheduling of energy requests into a shortest path problem, in which a dynamic programming (DP) algorithm is applied to achieve the global optimal solution.

A. Piecewise Optimal Strategy with Negligible Overhead

This subsection considers a simplified scenario where the overhead energy, e^r, is assumed negligible. We aim to mini-

mize the energy consumption at the ES in each piece of the feasible energy tunnel separately. Since the slope for the same piece is fixed, $E^b_{t_{r_i}}$ and E^r_i will remain unchanged and their subscripts can be dropped.

According to Property 1, in the case that the constant overhead, e^r, is negligible, an EHD harvests energy most efficiently when it requests a small amount of energy if and only if a quarter of maximum energy remains in the capacitor. Correspondingly, the following corollary is deduced.

Corollary 2: *For an optimal energy requesting strategy with negligible e^r, the EHD requests a tiny amount of energy from ES each time, when the residual energy is $\frac{1}{4}E^{eh}_m$, i.e, $E^r \to 0$ and $E^b = \frac{1}{4}E^{eh}_m$, if $e^r \to 0$.*

Corollary 2 forms the foundation to obtain the upper bound of a transmission rate for a capacitor-based EHD, which will be derived as follows.

From Corollary 2, the EHD cannot consume more energy during an energy request interval than the amount harvested in the last round, which is E^r. Combining this charging constraint with the constraint of the least energy requirement at the EHD, we have

$$\frac{E^r}{T^{es}\, p^{eh}} \geq 1, \tag{6}$$

where

$$T^{es} = RC \ln \left\{ \frac{\left(2E^{eh}_m\right)^{\frac{1}{2}} - \left(2E^b\right)^{\frac{1}{2}}}{\left(2E^{eh}_m\right)^{\frac{1}{2}} - \left[2\left(E^b + E^r\right)\right]^{\frac{1}{2}}} \right\}, \tag{7}$$

which is calculated from (4) and (5).

According to Corollary 2, substituting $E^b = \frac{1}{4}E^{eh}_m$ and $E^r \to 0$ into (6), the left side of the inequalities is a limit of the form $0/0$. Utilizing the continuously differentiable feature of T^{es} with respect to E^r and applying the L'Hôpital's rule on the left side of (6), we derive

$$\lim_{E^r \to 0} \frac{E^r}{T^{es}\, p^{eh}} = \lim_{E^r \to 0} \frac{1}{(T^{es})'\, p^{eh}} = \frac{E^{eh}_m}{2\,R\,C\,p^{eh}}, \tag{8}$$

where $(T^{es})'$ is the first order derivation of T^{es} with respect to E^r. Substituting (8) into (6), we obtain

$$p^{eh}(t) \leq \frac{E^{eh}_m}{2\,R\,C} = \frac{V^2_m}{4R}. \tag{9}$$

The right side of (9) is the highest power that a capacitor-based EHD could harvest from a dedicated ES. It reveals the upper bound of the energy consumption in a given time period regardless of the requesting strategy. Substituting (9) into the power-rate function, $g(\cdot)$, it yields an upper bound of the data transmission rate that a capacitor-based EHD can achieve.

B. Global Optimal Strategy

Due to the discrete feature of the harvested energy and the nonlinear relationship between the energy transmitted from an ES and that replenished to an EHD, the design of a global optimal strategy is a grand challenge. To tackle this challenge, we leverage the Graph theory to convert the optimal energy requesting design into a shortest path problem.

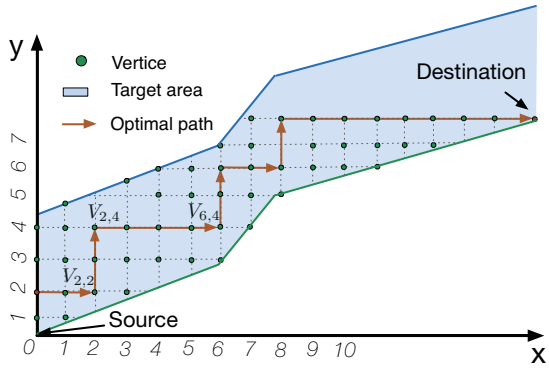

Fig. 5. The converted shortest path problem in a feasible energy tunnel.

As depicted in Fig. 5, assume the slope of each energy tunnel is smaller than the maximum transmission power in (9) that an EHD can afford, and then the area of the energy tunnel is divided into multiple grids uniformly. The intersections of the grids are referred to as "vertices" connected with horizontal and vertical "edges". Denote a vertex with the coordinates (j, k) by $V_{j,k}$, and the directed edge from $V_{j,k}$ to $V_{p,q}$ is represented by $e_{(j,k)\to(p,q)}$, where $\forall j, k, p, q \in \mathbb{Z}^+$. The length of the horizontal edge $e_{(j,k)\to(p,k)}$ represents the time interval between two successive energy harvests. Due to the charging constraint introduced in C3 of **P1**, the length of a lateral movement cannot be shorter than the charge time of the last energy replenishment, i.e., T^{es}_i, which is calculated through (7). A vertical edge $e_{(j,k)\to(j,q)}$ indicates an energy replenish by $E^r_i = y_q - y_k$, which generates an associate charging cost on an ES. We call this cost the weight of the edge, the calculation of which is specified by (5). The residual energy, $E^b_{t_{ri}}$ in (5), is measured in the vertical distance from y_k to the lower bound of the energy tunnel. A horizontal edge means no energy charging and has a weight of 0. Therefore, the weight of $e_{(j,k)\to(p,q)}$ is

$$w_{(j,k)\to(p,q)} = \begin{cases} 0, & j \neq p \text{ and } k = q, \\ E^{es}_i, & k \neq q \text{ and } j = p. \end{cases} \tag{10}$$

So far the second step of DTER has been converted into the classic single-pair shortest path problem in a directed and weighted graph. The source is a node with coordinates $(0, 0)$ and the destination is at the right end of the energy tunnel's lower boundary. It is not allowed to move backwards or downwards according to the features of EH process. Designing the optimal strategy for energy requesting is equivalent to finding the shortest path from the source to the destination such that the sum-weight of its constituent edges is minimized under the charging constraint. Consequently, the DP-based approach like Dijkstra's algorithm can be applied to schedule the optimal energy request scheme. The time complexity of such approach is $\mathcal{O}(n \log n)$, where n is the number of grids in the energy tunnel. More details of DP algorithms could be found in [26]. The solution accuracy heavily depends on the grid density in the graph, which will be evaluated from simulations.

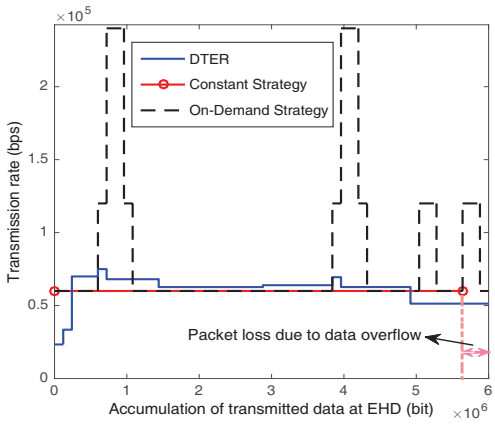

Fig. 6. Comparison of transmission rate at the EHD in a sample run.

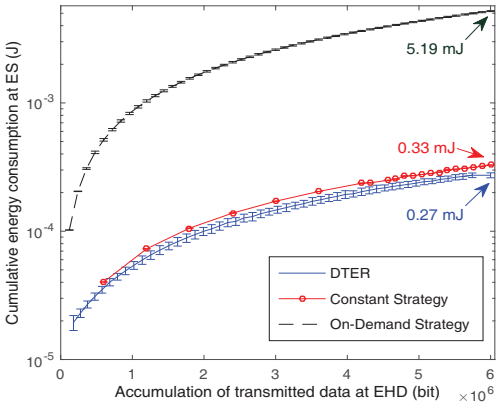

Fig. 7. Overall energy consumption among different strategies.

VII. Performance Evaluation

In this section, we conduct simulations to evaluate the performance of DTER and compare it with other energy requesting strategies. The simulation settings will be introduced first, and then the performance comparisons among different strategies are presented. Afterward, we study how different parameters affect the grid density of DTER to achieve the desired accuracy.

A. Simulation Settings

In the simulations, the central frequency and the bandwidth for data transmission are $f_d = 2.4\,\text{GHz}$ and $B = 50\,\text{kHz}$. Assume the wireless channel is AWGN and the noise spectrum density is $N_0 = -174\,\text{dBm}$; therefore, the noise power is $N_l = -127\,\text{dBm}$[2]. The distance from the EHD to its intended receiver is $d = 30\,\text{ft}$, and the propagation loss of an RF signal from EHD to the receiver is calculated through the free space path loss (FSPL) model, where

$$\text{FSPL}\,(\text{dB}) = 20\log_{10}(d) + 20\log_{10}(f_d) - 147.55. \quad (11)$$

According to the capacity of AWGN channel and propagation loss model, the power-rate function is

$$p^{eh}(\text{dBm}) = 10\log_{10}\left(2^{\frac{r^{eh}}{B}} - 1\right) + \text{FSPL} + N_l. \quad (12)$$

We assume the arrival of data packet is a Poisson process with a mean value λ. The size of each packet and the capacity of data storage are $S = 15\,\text{KB}$ and $D_m^{eh} = 64\,\text{KB}$. The maximum voltage, capacitance, and resistance of the EHD are $V_m = 2\,\text{V}$, $C = 2\,\text{nF}$, and $R = 1\,\text{k}\Omega$, respectively; therefore, the capacitor can store up to $E_m^{eh} = 4\,\text{nJ}$ of energy. The default overhead, e^r, of each energy request is $0.4\,\text{nJ}$, which is 10% of E_m^{eh}. The ES sends energy packets at a constant power of $p^{es} = 10\,\text{W}$[3]. The simulation results presented in this paper are based on the average of 70 independent runs, unless otherwise stated.

For comparison purpose, the performance of the following two representative power management strategies are also tested.

- *Constant strategy:* In this strategy, the EHD transmits data at a constant rate, which is λS. The data storage may overflow when a burst of data arrivers at the EHD in a short interval due to the randomness of data arrival. The EHD will request a energy replenishment and charge the capacitor to 75% of the maximum capacity, when the residual energy is not enough for a single packet transmission.
- *On-demand dynamic strategy:* To avoid the overflow of arriving data when the traffic rate has a sudden increase, the EHD adjusts its transmission rate adaptively based on the status of data storage — the higher occupancy of the storage, the higher transmission rate is applied. The occupancies of data storage and the corresponding transmission rates are $D^b = [1/16, 1/8, 1/4, 1/2, 3/4, 7/8, 15/16]$ and $r^{eh} = [1/8, 1/4, 1/2, 1, 2, 4, 8]\times\lambda S$. With this strategy, the EHD is scheduled to request adequate energy for the next data transmission.

B. Performance Comparison

In the performance comparison, we set the traffic generation rate as $\lambda = 0.5\,\text{pkt/s}$, and then compare the DTER with two alternative strategies in terms of transmission rate, packet loss ratio caused by the data overflow on the EHD, and energy consumption at the ES.

Fig. 6 demonstrates the transmission rate of the EHD under three strategies. According to Corollary 1 in Section IV, low transmission rate and small rate variation are helpful to reduce the energy consumed on data transmission. The constant strategy has the most stable transmission rate, thereby reducing the energy consumption of the EHD considerably. However, it has a significant data overflow problem since the arrivals of data packets are random but the constant strategy cannot adapt to the traffic dynamics. This can be observed in Fig. 6

[2] $N_l = N_0 + 10\log_{10}(B) = -127\,\text{dBm}$.

[3] p^{es} is determined by the input power and the output voltage of the EHD as introduced in [24]. The output voltage is 2 V if the receiving power is around $-10\,\text{dBm}$. Therefore, after considering the propagation loss, the required transmission power of the ES is around $40\,\text{dBm}$, i.e., $10\,\text{W}$.

where the accumulation of transmitted data with the constant strategy is less than the other two strategies. According to the measurement, due to the overflow of data storage, the average packet loss ratio of the constant strategy reaches 12.2%. In order to send packets timely, the on-demand strategy transmits at varying data rates depending on the occupancy rate of data storage. This causes frequent and drastic changes in the transmission rate at the EHD since there are large-scale fluctuations in the instantaneous arriving rate of data packets. On the contrary, the optimal transmission rate in DTER can adapt to the dynamic traffic while minimizing the variations in transmission rate without overflowing the data storage.

In Fig. 7, we compare the energy consumption amongst different strategies. Note that the logarithmic scale is employed for the y-axis due to the huge difference of absolute values. As shown in the figure, DTER has the least energy consumption among the three strategies, mainly for two reasons. First of all, DTER has the optimal transmission strategy at the EHD which guarantees the minimum energy consumption to send a given amount of data. Second, DTER implements the optimal energy requesting strategy which further reduces the energy consumption on ES. Although the results between the DTER and the constant strategy appear to be close to each other in the logarithmic scaled plot in Fig. 7, the actual energy consumption of the constant strategy is much higher than that of DTER, even at the cost of packet loss. More specifically, as shown in the figure, the average energy consumed at ES with the constant strategy is $0.33\,$mJ by the end of tests, 22% higher than that with DTER, which is $0.27\,$mJ. In contrast, the on-demand strategy mitigates the data overflow problem of the constant strategy, but consumes highest energy, which is $5.19\,$mJ at the ES due to the strong fluctuations in transmission rate and inefficient energy requests.

C. Analysis on Grid Density in DTER

In the simulations, Dijkstra's DP algorithm is applied to find the global optimal solution. When using such an approach in DTER, the computing accuracy, i.e., how close is the obtained result to the truly optimal solution, depends on the density of grids, which is defined as the number of grids in the unit area. The result converges to the global optimum energy consumption with the increase of grid density; an excessively high grid density, however, significantly increases the time complexity of the DP algorithm, but gives little if any accuracy improvement. Next, we study how different parameters affect the required density of the gird in DTER to reach a desired accuracy.

Obviously, in order to get a close result to the optimal solution, the length of vertical edge has to be smaller than the optimal E^r and the length of horizontal edge should be smaller than the time interval between neighboring energy requests in the optimal energy requesting strategy. Therefore, the parameters, e.g., λ and C, that affect E^r and the frequency of energy requests will also affect the required grid density.

As shown in Table. I, the increased λ results in a higher transmission rate and steeper feasible energy tunnel, which in turn increases the frequency of energy requests but does not significantly affect E^r. By contrast, a larger C will increase the energy replenished in each round and reduce the energy request frequency accordingly. Therefore, to achieve a certain accuracy, the required density of grid in DTER is proportional to λ but inversely proportional to C. This conclusion will be verified by the following simulations.

TABLE I
FREQUENCY AND AMOUNT OF ENERGY REQUEST

$C = 2\,$nF			$\lambda = 0.5\,$pkt/s		
λ	$\hat{E}^r$ ($10^{-10}\,$J)	Freq	C ($\,$nF$\,$)	$\hat{E}^r$ ($10^{-10}\,$J)	Freq
0.25	4.32	0.22	1	2.41	1.08
0.5	4.21	0.61	2	4.21	0.61
1	4.00	2.38	4	9.11	0.29

We define the improvement of accuracy as $(E^{es}_{\beta_{i+1}} - E^{es}_{\beta_i})/E^{es}_{\beta_i}$, where $\beta_0 = 5.25 \times 10^7$ is the initial grid density and $\beta_i = i\beta_0$ represents the grid density in the i^{th} iteration. In Fig. 8, we set the threshold of convergence as 0.5% of the accuracy improvement and show the cumulative distribution function (CDF) of grid density with respect to the packet generation rates, λ, capacitances, C, and the deadline of data transmission, T.

From Fig. 8, it can be observed that in DTER, both λ and C have a significant impact on the required density of grids to achieve the default accuracy, but the impact of T is negligible. Using CDF $= 0.9$ as an example, when $C = 2\,$nF but increase λ from 0.25 to 1, the required grid density increases from 3.4×10^9 to 1.2×10^{11}, as demonstrated in Fig. 8(a). When $\lambda = 0.5$ but increase C from $1\,$nF to $4\,$nF, the required grid density decreases from 6.5×10^{10} to 3.2×10^9, as shown in Fig. 8(b). When C and λ are fixed but change T from $50\,$s to $100\,$s, the required grid density remains unchanged, which is 9.4×10^9, as shown in Fig. 8(c). Therefore, the observations from Fig. 8 verify the previous conclusion, i.e., to achieve a certain accuracy, the required density of grid in DTER is proportional to λ but inversely proportional to C.

VIII. CONCLUSIONS

In this paper, we have presented an optimal energy requesting strategy, termed dual tunnel energy requesting (DTER), for RF-based energy harvesting wireless communication systems. The key feature of DTER is that both the charging feature of real energy storage components and the overhead issue of energy requests are taken into account to minimize the overall energy consumption. To solve the nonlinear optimization problem in DTER, the design of energy requesting strategy is converted into solving a classic shortest path problem, which enables us to find a global optimum solution through dynamic programming algorithms. We also conducted theoretical analysis and simulation study to evaluate the performance of DTER. This paper provides a lower bound of the overall energy consumption at both energy harvesting device and energy

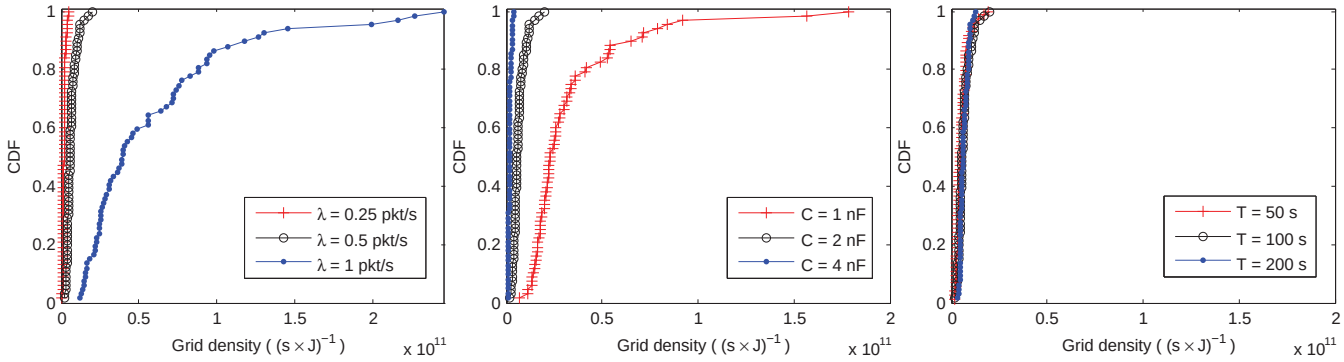

(a) Different traffic generation rates. (b) Different capacitances. (c) Different deadlines.

Fig. 8. CDF of grid density with different settings. (a) $C = 2\,\text{nF}$, $T = 100\,\text{s}$; (b) $\lambda = 0.5\,\text{pkt/s}$, $T = 100\,\text{s}$; (c) $C = 2\,\text{nF}$, $\lambda = 0.5\,\text{pkt/s}$.

source. The results sheds light on the future research of energy harvesting communications.

ACKNOWLEDGEMENT

The research of Yanxiao Zhao is supported in part by NSF ECCS-1310562. The research of Min Song is supported in part by NSF CNS-1526152 and CNS-1551067. Any opinion, finding, and conclusions expressed in this paper are those of the author and do not necessarily reflect the views of the National Science Foundation.

REFERENCES

[1] T. J. Kazmierski and S. Beeby, *Energy harvesting systems*. Springer, 2014.

[2] S. Ulukus, A. Yener, E. Erkip, O. Simeone, M. Zorzi, P. Grover, and K. Huang, "Energy harvesting wireless communications: a review of recent advances," *IEEE Journal on Selected Areas in Communications*, vol. 33, no. 3, pp. 360–381, 2015.

[3] S. Zhou, J. Gong, Z. Zhou, W. Chen, and Z. Niu, "GreenDelivery: proactive content caching and push with energy-harvesting-based small cells," *IEEE Communications Magazine*, vol. 53, no. 4, pp. 142–149, 2015.

[4] X. Lu, P. Wang, D. Niyato, and E. Hossain, "Dynamic spectrum access in cognitive radio networks with RF energy harvesting," *IEEE Wireless Communications*, vol. 21, no. 3, pp. 102–110, 2014.

[5] M. Piñuela, P. D. Mitcheson, and S. Lucyszyn, "Ambient RF energy harvesting in urban and semi-urban environments," *IEEE Transactions on Microwave Theory and Techniques*, vol. 61, no. 7, pp. 2715–2726, 2013.

[6] V. Liu, A. Parks, V. Talla, S. Gollakota, D. Wetherall, and J. R. Smith, "Ambient backscatter: wireless communication out of thin air," in *Proceedings of the Conference on Applications, Technologies, Architectures, and Protocols for Computer Communication (SIGCOMM)*. ACM, 2013, pp. 39–50.

[7] D. Mishra, S. De, S. Jana, S. Basagni, K. Chowdhury, and W. Heinzelman, "Smart RF energy harvesting communications: challenges and opportunities," *IEEE Communications Magazine*, vol. 53, no. 4, pp. 70–78, 2015.

[8] K. Kaushik, D. Mishra, S. De, S. Basagni, W. Heinzelman, K. Chowdhury, and S. Jana, "Experimental demonstration of multi-hop RF energy transfer," in *Proceedings of the International Symposium on Personal Indoor and Mobile Radio Communications (PIMRC)*. IEEE, 2013, pp. 538–542.

[9] K. Huang and V. K. Lau, "Enabling wireless power transfer in cellular networks: architecture, modeling and deployment," *IEEE Transactions on Wireless Communications*, vol. 13, no. 2, pp. 902–912, 2014.

[10] J. Yang and S. Ulukus, "Optimal packet scheduling in an energy harvesting communication system," *IEEE Transactions on Communications*, vol. 60, no. 1, pp. 220–230, 2012.

[11] K. Tutuncuoglu and A. Yener, "Optimum transmission policies for battery limited energy harvesting nodes," *IEEE Transactions on Wireless Communications*, vol. 11, no. 3, pp. 1180–1189, 2012.

[12] O. Orhan, D. Gunduz, and E. Erkip, "Throughput maximization for an energy harvesting communication system with processing cost," in *Proceedings of the Information Theory Workshop (ITW)*. IEEE, 2012, pp. 84–88.

[13] X. Lu, P. Wang, D. Niyato, and Z. Han, "Resource allocation in wireless networks with RF energy harvesting and transfer," *IEEE Network*, vol. 29, no. 6, pp. 68–75, 2015.

[14] R. Das and P. Harrop, "RFID forecasts, players and opportunities 2014–2024," *IDTechEx report*, 2014.

[15] M. Kaur, M. Sandhu, N. Mohan, and P. S. Sandhu, "RFID technology principles, advantages, limitations & its applications," *International Journal of Computer and Electrical Engineering*, vol. 3, no. 1, pp. 151–157, 2011.

[16] S. Percy, C. Knight, F. Cooray, and K. Smart, "Supplying the power requirements to a sensor network using radio frequency power transfer," *Sensors*, vol. 12, no. 7, pp. 8571–8585, 2012.

[17] K. Huang and X. Zhou, "Cutting the last wires for mobile communications by microwave power transfer," *IEEE Communications Magazine*, vol. 53, no. 6, pp. 86–93, 2015.

[18] X. Lu, P. Wang, D. Niyato, D. I. Kim, and Z. Han, "Wireless networks with RF energy harvesting: a contemporary survey," *IEEE Communications Surveys & Tutorials*, vol. 17, no. 2, pp. 757–789, 2015.

[19] M. Y. Naderi, P. Nintanavongsa, and K. R. Chowdhury, "RF-MAC: A medium access control protocol for re-chargeable sensor networks powered by wireless energy harvesting," *IEEE Transactions on Wireless Communications*, vol. 13, no. 7, pp. 3926–3937, 2014.

[20] O. Ozel, K. Tutuncuoglu, J. Yang, S. Ulukus, and A. Yener, "Transmission with energy harvesting nodes in fading wireless channels: optimal policies," *IEEE Journal on Selected Areas in Communications*, vol. 29, no. 8, pp. 1732–1743, 2011.

[21] M. Gorlatova, A. Wallwater, and G. Zussman, "Networking low-power energy harvesting devices: Measurements and algorithms," *IEEE Transactions on Mobile Computing*, vol. 12, no. 9, pp. 1853–1865, 2013.

[22] C. R. Valenta and G. D. Durgin, "Harvesting wireless power: survey of energy-harvester conversion efficiency in far-field, wireless power transfer systems," *IEEE Microwave Magazine*, vol. 15, no. 4, pp. 108–120, 2014.

[23] H. J. Visser and R. J. Vullers, "RF energy harvesting and transport for wireless sensor network applications: principles and requirements," *Proceedings of the IEEE*, vol. 101, no. 6, pp. 1410–1423, 2013.

[24] P. Nintanavongsa, U. Muncuk, D. R. Lewis, and K. R. Chowdhury, "Design optimization and implementation for RF energy harvesting circuits," *IEEE Journal on Emerging and Selected Topics in Circuits and Systems*, vol. 2, no. 1, pp. 24–33, 2012.

[25] Powercast Company, "Energy harvesting kid," powercastco.com. [Online]. Available: http://www.powercastco.com/products/development-kits/, [Accessed: June, 2016].

[26] M. Sniedovich, *Dynamic programming: foundations and principles*. CRC press, 2010.